

A NOVEL METHOD FOR RADAR INITIAL ORBIT DETERMINATION FROM ANGULAR TRACK AND DOPPLER SHIFT MEASUREMENTS

M.F. Montaruli⁽¹⁾, M.A. De Luca⁽¹⁾, P. Di Lizia⁽¹⁾, M. Massari⁽¹⁾, G. Bianchi⁽²⁾, G. Pupillo⁽²⁾, and M. Fiorentini⁽²⁾

⁽¹⁾*Department of Aerospace Science and Technology, Politecnico di Milano, Via G. La Masa 34, 20156, Milan, Italy, Email: {marcofelice.montaruli, mariaalessandra.deluca, pierluigi.dilizia, mauromassari}@polimi.it*

⁽²⁾*Istituto di Radioastronomia, Istituto Nazionale di Astrofisica, Via P. Gobetti 101, 40129, Bologna Italy, Email: {germano.bianchi, giuseppe.pupillo, matteo.fiorentini}@inaf.it*

ABSTRACT

The overpopulation of resident space objects requires an efficient space objects cataloguing capability. This paper describes a novel radar Initial Orbit Determination (IOD) algorithm when only angular track and Doppler shift measurements are available. First, a track compression is performed to derive the time derivative of the angular pair. An optical admissible region is computed, considering semi-major axis, range and eccentricity constraints. For bistatic radars, this region is converted to the bistatic plane. An admissible line is identified from the intersection of the admissible region with the measured range rate (derived from the Doppler shift) and then sampled, providing orbital state candidates. One of them enters a batch filter as first guess, from which the IOD result is returned.

The algorithm is validated using both numerical simulations and real data. The algorithm is applicable to any survey radar and offers greater reliability and ease of operational than existing methods.

Keywords: Space surveillance and tracking; Initial Orbit Determination; Admissible Regions; Space Surveillance Radars; Catalogue build-up and maintenance.

1. INTRODUCTION

Globally, the growing population of objects in orbit has become a major concern for space agencies and institutions, with Low Earth Orbit (LEO) and Geostationary Orbit (GEO) being the most affected regions. While only a small portion of these objects are active satellites, the majority are space debris, which pose a significant threat to space activities. To address this issue, an international effort is underway in the field of Space Surveillance and Tracking (SST), with the following services provided: conjunction analysis [1], fragmentation analysis [2] [3] and re-entry prediction [4].

All of these applications rely primarily on measurements derived from ground-based sensors, including tracking

and survey radars, which provide angular track, plus either slant range (SR) or Doppler shift (DS) measurements, or both. If a measurements track does not correlate to a catalogued object, the measurements are used alone to perform an Initial Orbit Determination (IOD).

Survey radars are theoretically capable of providing a robust IOD result even with tracks of only a few seconds in length, but on condition that angles and SR are present in the acquired measurements set [5] [6]. However, it is common that only angles and DS are provided by a radar system, like in the French GRAVES [7] and, for most operational scenarios, in the Italian BIRALES [14]. In this case, [8] proposes a method for reconstructing the SR profile based on Keplerian assumption and requiring long measurement tracks. However this is not the case for survey radars. Alternatively, the DAIOD algorithm presented in [9] solves the IOD problem by iteratively applying the Lambert's method and exploiting advanced computational techniques [10] [11].

The current work addresses the radar IOD problem when only angular and DS measurements are available by proposing a different paradigm. The resulting IODAD algorithm (Initial Orbit Determination from Angular and Doppler shift measurements) is based on the concepts of optical admissible regions [12]. This allows for more efficient use on short and noisy measurement tracks, making the proposed algorithm valid for processing data acquired by any survey radar. In addition, this approach does not exploit advanced computational techniques, providing greater flexibility and ease of operational application. The IODAD algorithm is described in Sec. 2, validated in Sec. 3 (numerically) and in Sec. 4 (real case scenario). The conclusions of the work are presented in Sec. 5.

2. IODAD ALGORITHM

The purpose of the IODAD algorithm is to perform IOD when, for an uncatalogued object, only angular track and DS measurements are available. The algorithm description is as follows.

First, the track compression is executed, at an observa-

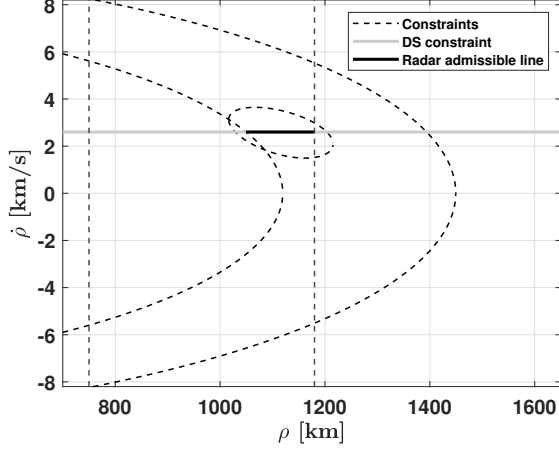


Figure 1: Radar admissible line for a monostatic system.

tion epoch specified by the user, returning the first time derivatives of the two angular coordinates [13]. These quantities are used together with the angular pair to compute an admissible region in the range ρ and range rate $\dot{\rho}$ plane [12]. The boundaries of such a region are defined according to the constraints given by the user in terms of energy (that is semi-major axis) and eccentricity [12]. Then, the flow forks depending on whether the radar is monostatic or bistatic.

In the monostatic case, the measured range rate $\dot{\rho}_{meas}$ can be directly related to the recorded DS through the following analytic equation:

$$\dot{\rho}_{meas} = \frac{c}{f_{TX}} DS \quad (1)$$

where c is the light velocity and f_{TX} is the transmitted frequency. By this way, it is possible to add the following constraint to the admissible region:

$$|\dot{\rho} - \dot{\rho}_{meas}| \leq \eta \quad (2)$$

where η is a threshold quantity which can be defined, for instance, based on the DS measurement resolution of the sensor. Since surveillance radars usually provide a good DS resolution, η can be set equal to zero. The new admissible region turns out to be a straight line, as the measured $\dot{\rho}_{meas}$, analytically derived from the recorded DS, is considered as the only admissible $\dot{\rho}$ value, and multiple possible ρ values are compliant with it, as shown in Fig. 1. This operation provides $\langle \rho, \dot{\rho} \rangle$ candidate pairs, which can be used to compute a set of Virtual Debris (VDs). These VDs represent possible orbital states of the observed target.

For a bistatic radar system instead, the DS measurement is related to the bistatic SR derivative, that is the deriva-

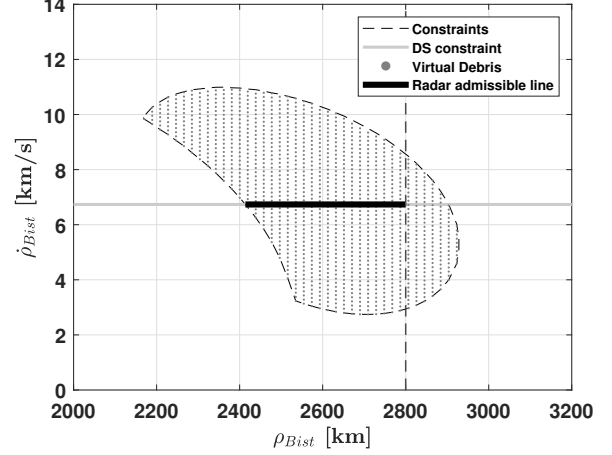


Figure 2: Radar admissible line for a bistatic system.

tive of the sum between ρ_{TX} (distance transmitter-target) and ρ_{RX} (distance target-receiver). Thus, the admissible region defined according to energy and eccentricity constraints is first sampled to compute the VDs according to a uniform grid. Starting from the orbital state of each VD, both bistatic SR (ρ_{Bist}) and bistatic SR derivative ($\dot{\rho}_{Bist}$) are then simulated. At this point, Eq. 2 is evaluated, selecting a term η compatible with the $\dot{\rho}_{Bist}$ resolution. In this case η must be non-zero to guarantee the presence of VDs in the computed radar admissible line. Figure 2 shows the admissible region on the bistatic plane, which is derived from the monostatic case represented in Fig. 1. At this point, only the VDs satisfying the distance constraint (maximum SR) and the condition in Eq. 2 are retained.

At this stage, for both the monostatic and bistatic pipelines, a VD is selected as first guess \mathbf{x}_0 and fed to a batch filter to compute an IOD result, both in terms of mean state \mathbf{x} and covariance \mathbf{P} . The first guess \mathbf{x}_0 is selected as the minimum eccentricity VD, since the target is likely to be a LEO object.

3. NUMERICAL SIMULATION

The IODAD algorithm presented in Sec. 2 is here tested against a synthetic data set of measurements. Such a data set is retrieved by simulating observations of the Bistatic Radar for LEO Survey (BIRALES), an Italian bistatic radar system devoted to space surveillance [14] [15] [16] [17]. In BIRALES a Continuous Wave (CW) system is used to obtain DS and angular track measurements. It should be remarked that BIRALES sensor is only used as a baseline, as the proposed approach is valid for any survey radar.

A synthetic data set composed of 413 transits related to 395 objects from the NORAD catalogue [18] is analysed.

	p_{err} [km]	v_{err} [km/s]
0%	1.1e-01	1.6e-03
25%	2.7e+00	8.5e-03
50%	4.7e+00	1.4e-02
75%	7.8e+00	2.5e-02
100%	2.1e+02	8.8e-01

Table 1: Nominal numerical analysis for the bistatic case: IODAD performance in terms of the 0%, 25%, 50%, 75% and 100% percentiles.

RMSE _{Az} [deg]	RMSE _{El} [deg]	RMSE _{Ds} [km/s]	duration [s]
3.8e-01	5.2e-02	3.0e-02	2.5e+01

Table 2: Real case scenario: measurement characteristics.

Ground truth trajectory is generated by a SGP4 propagation, and noise is associated to the measurements: 1e-02 deg on the angular track and 7e-03 km/s (equivalent to about 10 Hz in frequency) on the DS measurements. Concerning the admissible regions boundaries, the maximum eccentricity is set equal to 0.35, the minimum semi-major axis to 6378 km, the maximum semi-major axis to 106378 km, and the maximum slant range to 3100 km. The simulation results are reported in Tab. 1, in terms of position and velocity errors with respect to the ground truth. It is worth to notice that the accuracy depends on the measurement track length, the acquisition frequency and the noise level. A sensitivity analysis (not reported in this paper) on the sampling frequency and on the measurements noise proves that the IODAD algorithm is valid for any survey radar. In general, these analyses demonstrate the accuracy and reliability of the method.

4. REAL CASE SCENARIO

The IODAD algorithm described in Sec. 2 is tested on a BIRALES real observation of the SARAL satellite (Norad ID 39086), whose ephemerides are provided by the International Laser Ranging Service (ILRS). Table 2 illustrates the measurement characteristics of the transit, including the Root Mean Square Error (RMSE), with respect to the transit prediction, for azimuth, elevation and DS. Also, the duration of the measurement track is reported. To better assess the potential of the IODAD algorithm, the same observation is processed by the IOD algorithm presented in [8] (introduced in Sec. 1).

The results are reported in Tab. 3. It can be seen that IODAD performance is consistent with the numerical simulations in Sec. 3. In addition, IODAD presents significantly better performance with respect to the method in [8]. Overall, the test proves the reliability of the IODAD algorithm in real applications.

	p_{err} [km]	v_{err} [km/s]
IODAD	8.2e-01	1.9e-01
Reference	8.8e+02	7.5e+00

Table 3: Real case scenario: IODAD performance. Also the results of the IOD algorithm presented in [8], taken as reference, are reported

5. CONCLUSIONS

This work presented the IODAD algorithm, which is an innovative radar initial orbit determination method when angular track and Doppler shift measurements are available. Unlike existing methods, the new algorithm offers greater flexibility and ease of operational application, as it does not need long measurement tracks as input, nor a specific advanced computational technique.

Both numerical simulations and real case scenarios prove the potential of the IODAD algorithm. In particular, the algorithm performs significantly better than the existing method used as term of comparison.

As a future step, an extensive validation campaign on real data will be conducted to test the performance of the IODAD algorithm.

6. ACKNOWLEDGEMENT

The research activities described in this paper were carried out with the contribution of the NextGenerationEU funds within the National Recovery and Resilience Plan (PNRR), Mission 4—Education and Research, Component 2— From Research to Business (M4C2), Investment Line 3.1—Strengthening and creation of Research Infrastructures, Project IR0000026 – Next Generation Croce del Nord - Project Identification Code (CUP) C53C22000880006.

REFERENCES

1. S. Bonaccorsi, M.F. Montaruli, P. Di Lizia, M. Peroni, A. Panico, M. Rigamonti, F. Del Prete, Conjunction Analysis Software Suite for Space Surveillance and Tracking, *Aerospace* 2024, 11, 122. <https://doi.org/10.3390/aerospace11020122>
2. M.F. Montaruli, P. Di Lizia, E. Cordelli, H. Ma, J. Siminski, A stochastic approach to detect fragmentation epoch from a single fragment orbit determination, *Advances in Space Research*, Volume 72, Issue 9, 2023, <https://doi.org/10.1016/j.asr.2023.08.031>.
3. A. Muciaccia, L. Facchini, M.F. Montaruli, G. Purpura, R. Detomaso, C. Colombo, M. Mas-sari, P. Di Lizia, A. Di Cecco, L. Salotti, G. Bianchi, Radar observation and reconstruction of Cosmos 1408 fragmentation, *Journal of Space Safety Engineering*, Volume 11, Issue 1, 2024, <https://doi.org/10.1016/j.jsse.2023.11.006>.

4. M.F. Montaruli, L. Facchini, N. Faraco, P. Di Lizia, M. Massari, G. Bianchi, C. Bortolotti, A. Maccaferri, M. Roma, M. Peroni, L. Salotti, E. Vellutini, Third Long-March 5B re-entry campaign through Italian space surveillance radars, *Advances in Space Research*, Volume 75, Issue 2, 2025, <https://doi.org/10.1016/j.asr.2024.11.076>.
5. J. Siminski, Techniques for assessing space object cataloguing performance during design of surveillance systems. In: 6th International Conference on Astrodynamics Tools and Techniques (ICATT), 2016.
6. J.M. Montilla, J. Siminski, R. Vazquez, Single track orbit determination analysis for low Earth orbit with approximated J2 dynamics, *Advances in Space Research*, Volume 74, Issue 10, 2024, <https://doi.org/10.1016/j.asr.2024.09.035>.
7. A. Jouadé, A. Barka, Massively Parallel Implementation of FETI-2LM Methods for the Simulation of the Sparse Receiving Array Evolution of the GRAVES Radar System for Space Surveillance and Tracking, in *IEEE Access*, vol. 7, pp. 128968-128979, 2019, <https://doi.org/10.1109/ACCESS.2019.2938011>.
8. C. Yanez, F. Mercier, J.C. Dolado, A Novel Initial Orbit Determination Algorithm from Doppler and Angular Observations, In: 7th European Conference on Space Debris, 2017.
9. M. Losacco, R. Armellin, C. Yanez, L. Pirovano, S. Lizy-Destrez and F. Sanfedino, Robust Initial Orbit Determination for Surveillance Doppler-Only Radars, *IEEE Transactions on Aerospace and Electronic Systems*, vol. 59, no. 5, pp. 5000-5011, 2023, <https://doi.org/10.1109/TAES.2023.3249667>.
10. R. Armellin, P. Di Lizia, Probabilistic Optical and Radar Initial Orbit Determination, *Journal of Guidance, Control, and Dynamics*, 2018 41:1, 101-118, <https://doi.org/10.2514/1.G002217>.
11. A. Wittig, P. Di Lizia, R. Armellin, Propagation of large uncertainty sets in orbital dynamics by automatic domain splitting, *Celest Mech Dyn Astr* 122, 239-261 (2015). <https://doi.org/10.1007/s10569-015-9618-3>.
12. A. Milani, G.F. Gronchi, M. De' Michieli Vitturi, Z. Knezevic, Orbit determination with very short arcs. I admissible regions. *Celestial Mech Dyn Astr* 90, 57-85 (2004). <https://doi.org/10.1007/s10569-004-6593-5>.
13. A. Pastor, M. Sanjurjo-Rivo, D. Escobar, Track-to-track association methodology for operational surveillance scenarios with radar observations, *CEAS Space Journal*, 15, 535-551, 2023, <https://doi.org/10.1007/s12567-022-00441-4>.
14. M.F. Montaruli, L. Facchini, P. Di Lizia, M. Massari, G. Pupillo, G. Bianchi, G. Naldi, Adaptive track estimation on a radar array system for space surveillance, *Acta Astronautica*, Volume 198, 2022, Pages 111-123, <https://doi.org/10.1016/j.actaastro.2022.05.051>.
15. M.F. Montaruli, M.A. De Luca, M. Massari, G. Bianchi, A. Magro, Operational Angular Track Reconstruction in Space Surveillance Radars through an Adaptive Beamforming Approach. *Aerospace* 2024, 11, 451. <https://doi.org/10.3390/aerospace11060451>
16. M.F. Montaruli, P. Di Lizia, S. Tebaldini, G. Bianchi, Adaptive track approach for multiple sources scenarios during radar survey for space surveillance applications, *Aerospace Science and Technology*, Volume 152, 2024, <https://doi.org/10.1016/j.ast.2024.109307>.
17. M.F. Montaruli, P. Di Lizia, S. Tebaldini, G. Bianchi, Delta-k approach for space surveillance multireceiver radars, 2024, *Astrodynamics*, <https://doi.org/10.1007/s42064-024-0217-5>
18. D. A. Vallado, P. Crawford, R. Hujsak, T.S. Kelso, Revisiting Spacetrack Report \#3!, *AIAA Astrodynamics Specialists Conference and Exhibit* 2006